JCTC Journal of Chemical Theory and Computation

Article

pubs.acs.org/JCTC

Removal of Basis-Set Artifacts in Kohn−Sham Potentials Recovered from Electron Densities

Alex P. Gaiduk, Ilya G. Ryabinkin, and Viktor N. Staroverov*

Department of Chemistry, The University of Western Ontario, London, Ontario N6A 5B7, Canada

ABSTRACT: Kohn−Sham effective potentials recovered from Gaussian-basis-set electron densities exhibit large oscillations and asymptotic divergences not found in exact potentials and in functional derivatives of approximate density functionals. We show that the detailed structure of these oscillations and divergences is almost exclusively determined by the basis set in terms of which the reference density is expressed, and is almost independent of the density-functional or wave function method used for computing the density. Based on this observation, we propose a smoothening scheme in which most basis-set artifacts in a Kohn−Sham potential recovered from a given density are removed by subtracting the oscillation profile of the exchange-only local-density approximation potential computed in the same basis set as the reference density. The correction allows one to obtain smooth Kohn−Sham potentials from electron densities even for small Gaussian basis sets and greatly reduces discrepancies between the original (input) density and the density obtained from the reconstructed potential.

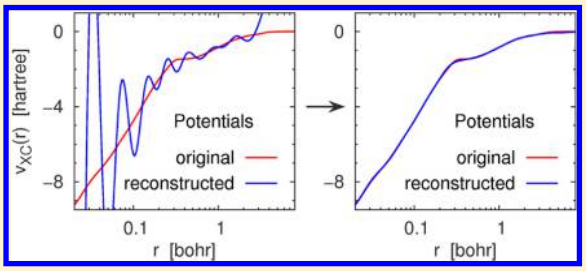

1. INTRODUCTION

The problem of constructing the Kohn−Sham effective potential corresponding to a given electron density arises in a number of applications of modern density-functional theory (DFT).[1−3] In basic DFT, Kohn−Sham potentials determined from accurate *ab initio* electron densities are used as benchmarks for developing model exchange-correlation potentials[4−8] and energy functionals.[9−14] In applied DFT, Kohn−Sham inversion is a key step of various density-embedding (partition) schemes.[15−20]

A variety of numerical methods for determining the Kohn−Sham potential from a given electron density of a many-electron system have been proposed in the literature (see, for instance, refs 21−29 and references therein). When applying these methods, several workers[23,30,31] observed that if the input density is taken from an *ab initio* or density-functional calculation employing a Gaussian-type basis set, the resulting Kohn−Sham potential exhibits large unphysical oscillations and asymptotic divergences that are not present either in exact Kohn−Sham potentials or in explicitly evaluated functional derivatives of approximate density functionals. These oscillations and divergences are *not* results of numerical errors but genuine consequences of subtle inaccuracies of electron densities expressed in terms of Gaussian-type basis functions.[23,30]

One way to reduce the severity of basis-set artifacts in Kohn−Sham potentials recovered from electron densities is to use basis sets of a very large size.[23,30,31] However, this approach is impractical in most real-life situations. Besides, use of large Gaussian-type basis sets only masks the problem instead of solving it: the oscillations are pushed into the core-electron region, while asymptotic divergences shift farther out in the periphery.

In this work, we propose an alternative remedy: a correction (smoothening) procedure that effectively eliminates oscillations and divergences in Kohn−Sham potentials recovered from Gaussian-basis-set densities. We also show that the corrected (smoothened) reconstructed potentials reproduce the original densities (and hence energies) much better than the raw reconstructed potentials.

2. KOHN−SHAM INVERSION

For the purpose of explaining our approach, we will assume, without loss of generality, that the occupied canonical Kohn−Sham orbitals and orbital energies corresponding to the reference density $\rho(\mathbf{r})$ are somehow already known. Then, the exchange-correlation potential corresponding to $\rho(\mathbf{r})$ can be obtained as follows.

Start with the usual Kohn−Sham equations

$$\left[-\frac{1}{2}\nabla^2 + v_{\text{eff}}(\mathbf{r})\right]\phi_i(\mathbf{r}) = \varepsilon_i\phi_i(\mathbf{r}) \tag{1}$$

where $v_{\text{eff}}(\mathbf{r})$ is the Kohn−Sham effective potential, $\phi_i(\mathbf{r})$ is the spatial part of the ith canonical Kohn−Sham spin-orbital, and ε_i is its eigenvalue. Multiply eq 1 by $\phi_i^*(\mathbf{r})$, sum over the occupied orbitals, and divide through by $\rho(\mathbf{r}) = \sum_{i=1}^{N} |\phi_i(\mathbf{r})|^2$. The result may be written as

$$v_{\text{eff}}(\mathbf{r}) = \frac{1}{\rho(\mathbf{r})}\sum_{i=1}^{N}\left[\frac{1}{2}\phi_i^*(\mathbf{r})\nabla^2\phi_i(\mathbf{r}) + \varepsilon_i|\phi_i(\mathbf{r})|^2\right] \tag{2}$$

The exchange-correlation potential $v_{\text{XC}}(\mathbf{r})$ is then given by the difference

$$v_{\text{XC}}(\mathbf{r}) = v_{\text{eff}}(\mathbf{r}) - v(\mathbf{r}) - v_{\text{H}}(\mathbf{r}) \tag{3}$$

Received: May 19, 2013
Published: July 15, 2013

where $v(\mathbf{r})$ is the external potential for the system and $v_H(\mathbf{r})$ is the Hartree (electrostatic) potential of $\rho(\mathbf{r})$. Equations 2 and 3 enable one to "reverse-engineer" the exchange-correlation potential $v_{XC}(\mathbf{r})$ from its canonical Kohn–Sham orbitals and eigenvalues in a single step.[21,32,33]

One might suppose that the potential $v_{eff}(\mathbf{r})$ can be also obtained by inverting eq 1 for any particular Kohn–Sham orbital. In practice, however, such orbital-specific inversion is possible only for the nodeless (lowest occupied) orbital, and even then, it is plagued by severe numerical difficulties.[34] For example, potentials recovered from core orbitals expanded in Gaussian basis sets would be essentially nonsensical because Gaussian basis functions fall off too quickly. Equation 2, which can be thought of as a weighted average of potentials obtained by inverting eq 1 for individual occupied orbitals,[33] avoids most of those difficulties and so is much better suited for calculations on many-electron systems.

Because the Kohn–Sham inversion formula (eq 2) was derived simply by rearranging the Kohn–Sham equations, one may assume that it should return the potential $v_{XC}(\mathbf{r})$ used to generate $\{\phi_i\}$ and $\{\varepsilon_i\}$ in the first place. In reality, the expected result is obtained only in a complete basis set. In calculations with finite basis sets (especially of the Gaussian type), the right-hand side of eq 3 does not recover the $v_{XC}(\mathbf{r})$ that went into eq 1, but produces a distinct potential.[23,30,31,34]

Let us illustrate this important point by the example of an exchange-only local-density approximation (LDA-X) calculation on a Ne atom. Using the *Gaussian* code,[35] we have solved the Kohn–Sham equations within the self-consistent-field (SCF) LDA-X scheme using the 6-311G basis set (a [4*s*,3*p*] contraction for Ne). Then, we constructed the LDA-X potential in two ways: by definition as

$$v_X^{LDA}(\mathbf{r}) = -\left(\frac{3}{\pi}\right)^{1/3}\rho^{1/3}(\mathbf{r}) \tag{4}$$

and by substituting the self-consistent eigenfunctions and eigenvalues of the LDA-X Hamiltonian into the Kohn–Sham inversion formula. The results are drastically different (Figure 1).

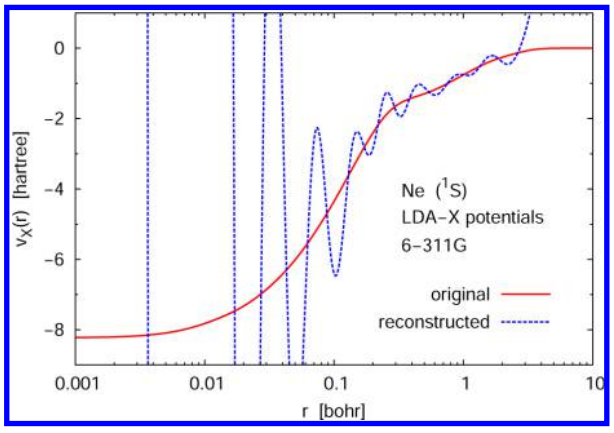

Figure 1. Exchange potentials obtained by eq 4 (original) and by eqs 2 and 3 (reconstructed) using the SCF solutions of the LDA-X Kohn–Sham equations in the 6-311G basis set.

The LDA-X potential obtained by eq 4 is smooth and tends to zero as $r \to \infty$, whereas the potential obtained by Kohn–Sham inversion oscillates (with frequency and amplitude increasing toward the nucleus) and diverges at large r.

The same calculation repeated with the universal Gaussian basis set[36] (UGBS), a large primitive basis set of the composition (23*s*,16*p*) for the Ne atom, produces somewhat different results (Figure 2). The oscillations of the reconstructed LDA-X potential are now confined to the vicinity of the nucleus ($r < 0.1$ bohr), and the potential itself begins to diverge only at $r \approx 6$ bohr. In the range between 0.1 and 6 bohr, the original and reconstructed LDA-X potentials coincide.

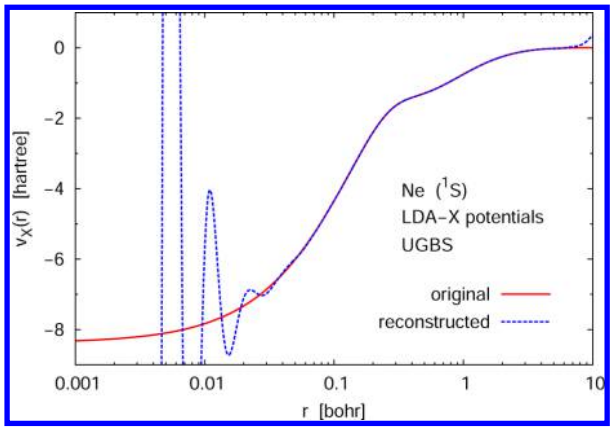

Figure 2. Same as in Figure 1 except that the Kohn–Sham orbitals and orbital energies were obtained using a very large basis set (UGBS).

The oscillations and asymptotic divergences observed in Figures 1 and 2 are purely deterministic, and their origin is well understood.[23] The oscillations arise from minute undulations of the Kohn–Sham orbitals that are amplified by differentiation and transferred to the Kohn–Sham potential via the Laplacian-dependent terms $\phi_i^*\nabla^2\phi_i$ of eq 2. The magnitude of the oscillations decreases with increasing basis set size because large basis sets represent Kohn–Sham orbitals and $\rho(\mathbf{r})$ more accurately. This is why the original and reconstructed LDA-X potentials obtained in a large basis (UGBS) are much closer to each other than the same potentials obtained in a small basis (6-311G). As for the asymptotic divergences, they are due to the fact that Gaussian functions fall off much faster than the exponentially decaying exact electron density. From this, it is easy to deduce[23,30] that the potential reconstructed from a Gaussian-basis-set density must diverge quadratically.[37]

3. OSCILLATION PROFILES

To compare the oscillatory features of Kohn–Sham potentials recovered from various electron densities, it is convenient to introduce an *oscillation profile*, which we define as

$$\Delta v_{osc}(\mathbf{r}) = v_{reconstructed}(\mathbf{r}) - v_{original}(\mathbf{r}) \tag{5}$$

where $v_{original}(\mathbf{r})$ is the potential analytically computed for a given density and $v_{reconstructed}(\mathbf{r})$ is the potential obtained from the same density by inverting the Kohn–Sham equations. By comparing oscillation profiles of Kohn–Sham potentials recovered from various electron densities, we found that the structure of oscillations of $v_{reconstructed}(\mathbf{r})$ is nearly identical for all densities obtained in the same basis set even when the levels of theory used for generating those densities are different.

Consider, for instance, the following three types of potentials: the LDA-X potential, the exchange part of the model potential of van Leeuwen and Baerends[21] (LB94-X), and the functional derivative of the Perdew–Burke–Ernzerhof[39] exchange-correlation (PBE-XC) functional. The oscillation

dx.doi.org/10.1021/ct4004146 | J. Chem. Theory Comput. 2013, 9, 3959–3964

profiles of these potentials computed with the 6-311G basis set are strikingly similar (Figure 3). This similarity increases with

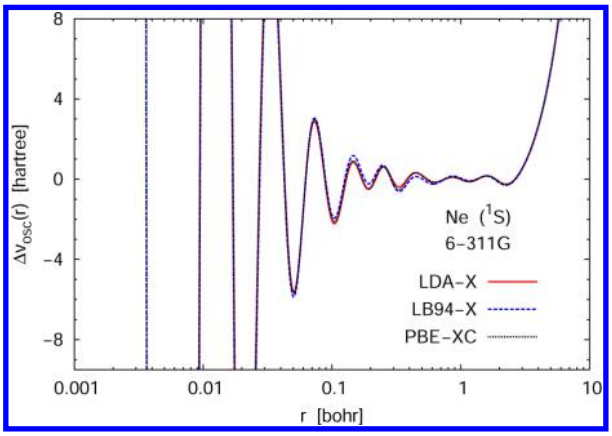

Figure 3. Oscillation profiles of Kohn−Sham potentials corresponding to various electron densities generated using the 6-311G basis set.

the basis set size and, for the nearly saturated UGBS, the three profiles become virtually identical (Figure 4).

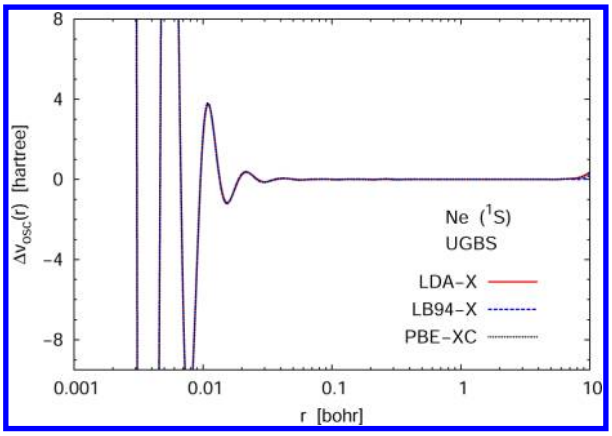

Figure 4. Same as in Figure 3 except that the densities were obtained using a very large basis set (UGBS).

The following observation appears to hold true in general: if two electron densities for a given system are computed with different density functionals but the same basis set, the oscillation profiles of the corresponding reconstructed Kohn−Sham potentials almost coincide.

The oscillation profile is related to a measure of basis set incompleteness called the "orbital error function", which was studied by Schipper et al.[23] For basis-set solutions of the Kohn−Sham equations, this function is defined as the difference between the left- and right-hand sides of eq 1,

$$\delta_i(\mathbf{r}) = \left[-\frac{1}{2}\nabla^2 + v_{\text{eff}}(\mathbf{r})\right]\phi_i(\mathbf{r}) - \varepsilon_i\phi_i(\mathbf{r}) \tag{6}$$

It is not difficult to see that our oscillation profile is a weighted average of orbital error functions,

$$\Delta v_{\text{osc}}(\mathbf{r}) = -\frac{1}{\rho(\mathbf{r})}\sum_{i=1}^{N}\phi_i^*(\mathbf{r})\delta_i(\mathbf{r}) \tag{7}$$

In a complete basis set, each $\delta_i(\mathbf{r})$, and hence $\Delta v_{\text{osc}}(\mathbf{r})$, would vanish.

4. SMOOTHENING SCHEME

The fact that oscillation profiles for different approximations are similar suggests the following smoothening procedure. Suppose we have a set of canonical Kohn−Sham orbitals and orbital eigenvalues corresponding to some unknown effective potential. We can recover this potential using eq 3, but $v_{\text{reconstructed}}(\mathbf{r})$ will generally contain spurious features. As we showed in the preceding section, an oscillation profile is a characteristic of the basis set, not of the density-functional approximation. Therefore, we can precompute the oscillation profile for some known potential and then subtract it from the reconstructed potential of interest.

The simplest way to generate an oscillation profile for a given basis set is by using the SCF LDA-X scheme. The smoothened (corrected) potential can then be obtained as

$$v_{\text{corrected}}(\mathbf{r}) = v_{\text{reconstructed}}(\mathbf{r}) - \Delta v_{\text{osc}}^{\text{LDA-X}}(\mathbf{r}) \tag{8}$$

where $\Delta v_{\text{osc}}^{\text{LDA-X}}$ is the oscillation profile of the self-consistent LDA-X potential.

Consider an example. We have solved the Kohn−Sham equations for the Ne atom using the PBE-XC functional and the 6-311G basis set. The potential $v_{\text{original}}(\mathbf{r})$, which was obtained by substituting the PBE-XC/6-311G density into the analytic expression for the functional derivative of the PBE-XC functional, is a smooth curve. The potential $v_{\text{reconstructed}}(\mathbf{r})$, obtained by Kohn−Sham inversion, is highly oscillatory (left panel in Figure 5). After subtracting the LDA-X/6-311G

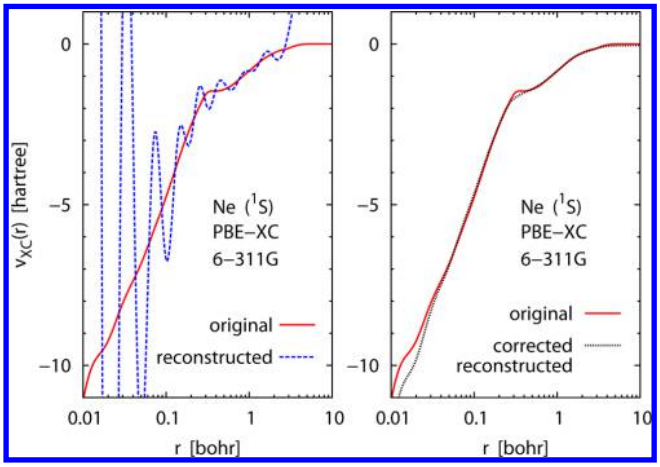

Figure 5. Original and reconstructed PBE-XC potentials for the Ne atom obtained using the 6-311G basis set. The reconstructed potentials are shown before (left panel) and after (right panel) subtracting the LDA-X/6-311G oscillation profile.

oscillation profile, the oscillations and asymptotic divergence disappear (right panel in Figure 5). Note that the corrected reconstructed PBE-XC potential is close, but not completely identical, to $v_{\text{original}}(\mathbf{r})$, because the 6-311G basis is small.

The procedure works even better for large basis sets such as UGBS, where the agreement between the original and corrected reconstructed PBE-XC potentials is nearly perfect (Figure 6).

The proposed smoothening scheme is especially effective in calculations with fully uncontracted Pople-style Gaussian basis sets. A typical example involving the PBE-XC potential and the uncontracted 6-311G (u-6-311G) basis set is shown in Figure 7.

dx.doi.org/10.1021/ct4004146 | J. Chem. Theory Comput. 2013, 9, 3959−3964

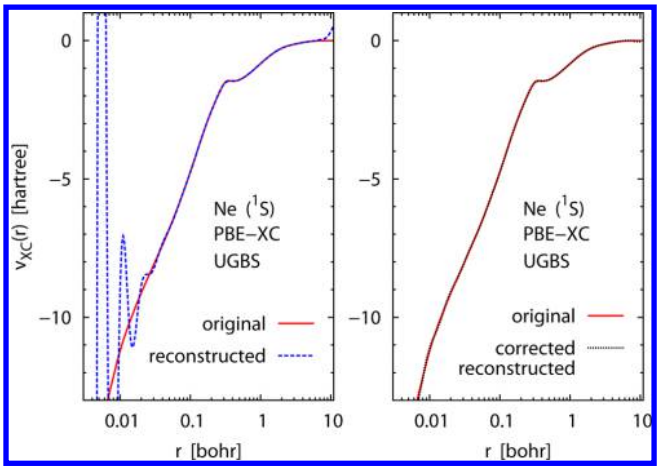

Figure 6. Same as in Figure 5 except that the density, the original potential, and the LDA-X oscillation profile were all computed using a very large basis set (UGBS).

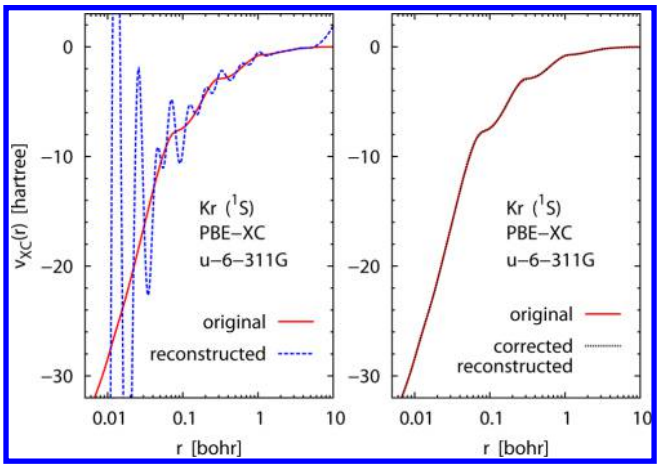

Figure 7. Original and reconstructed PBE-XC potentials for the Kr atom obtained using the uncontracted (u-) 6-311G basis set. The reconstructed potentials are shown before (left panel) and after (right panel) subtracting the LDA-X/u-6-311G oscillation profile.

Here, the corrected reconstructed PBE-XC potential almost exactly matches the original PBE-XC potential. Similarly excellent results were also obtained for the Ne, Mg, and Ar atoms (not shown).

The method can be applied to molecules with equal ease. An example involving the PBE-XC potential for the ground-state CO molecule computed with the uncontracted 6-311G* (u-6-311G*) basis set is shown in Figure 8. Here, as before, subtraction of the LDA-X oscillation profile causes dramatic improvement in the shape of the reconstructed PBE-XC potential. The only discrepancy concerns the small peaks that are seen in $v_{\text{original}}(\mathbf{r})$ on the shoulders of the C and O potential wells but are missing in the smoothened potential. A similar effect was noted in Figure 5 for the smoothened PBE-XC/6-311G potential of the Ne atom. These minor discrepancies are due to basis-set incompleteness. For the Ne atom, a switch from the 6-311G basis to the UGBS was enough for the peak to appear (right panel in Figure 6). For the CO molecule, the peaks started to emerge only when we used the UGBS3P basis (UGBS augmented with 3 sets of polarization functions for each exponent[40]). Similar results were obtained for the N_2 molecule (not shown).

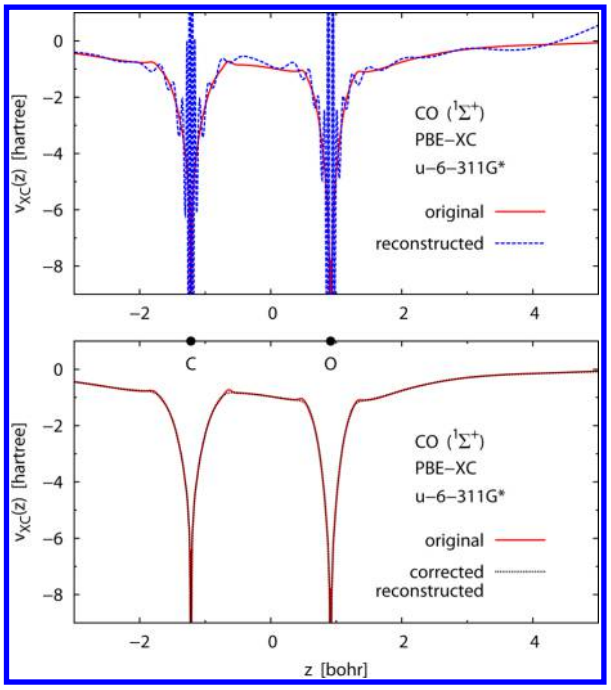

Figure 8. Original and reconstructed PBE-XC potentials for the CO molecule obtained using the uncontracted 6-311G* basis set. The reconstructed potentials are shown along the internuclear axis before (upper panel) and after (lower panel) subtracting the LDA-X/u-6-311G* oscillation profile. The CO distance is set at the experimental equilibrium bond length (r_e = 2.132 bohr).

The basic idea of our method—calculation and subtraction of a known oscillation profile from an oscillatory potential—is not limited to Kohn–Sham inversion methods where $v_{\text{reconstructed}}(\mathbf{r})$ is obtained by eq 2 in a single step. The same approach can be combined with *any* density-to-potential mapping technique such as the methods of Zhao, Morrison, and Parr,[24] van Leeuwen and coworkers,[21,22] Wu and Yang,[26] Jacob,[31] Ryabinkin and Staroverov,[29] and others.

To illustrate how our correction scheme works in situations where the Kohn–Sham orbitals and orbital energies corresponding to $\rho(\mathbf{r})$ are unknown *a priori*, we resorted to our recent density-to-potential mapping method,[29] which is based on the differential virial theorem for noninteracting electrons.[41−43] First, we obtained the Hartree–Fock (HF) electron density of the Ar atom using the UGBS and then calculated the exchange-correlation potential corresponding to this density by the method of ref 29. Figure 9 shows that the resulting potential has large oscillations near the nucleus and diverges asymptotically. Note that the oscillatory structure of this $v_{\text{reconstructed}}(\mathbf{r})$ is already similar to that of the LDA-X/UGBS potential shown in Figure 1. Then, we computed LDA-X/UGBS density for the same system, reconstructed the corresponding LDA-X potential (also by the method of ref 29), and subtracted the analytic LDA-X potential to obtain the LDA-X oscillation profile. After this profile was subtracted from the raw potential recovered from the HF/UGBS density, we obtained an essentially exact $v_{\text{XC}}(\mathbf{r})$ (Figure 9).

5. EFFECT OF THE CORRECTION ON DENSITIES AND ENERGIES

As shown in ref 31, a Kohn–Sham potential reconstructed from a given $\rho_{\text{input}}(\mathbf{r})$ can reproduce the input density exactly only when the Kohn–Sham equations with that potential are solved

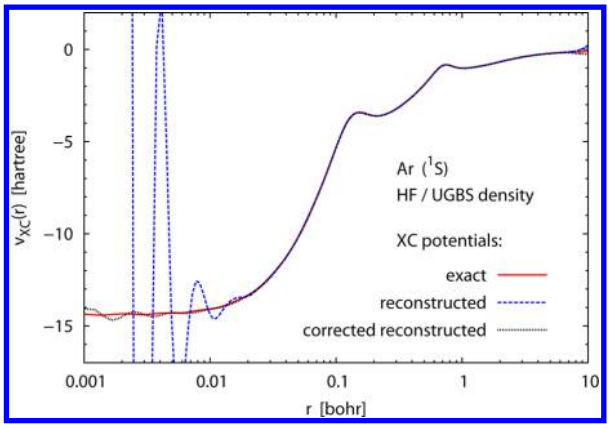

Figure 9. Exchange-correlation potentials reconstructed from the HF/UGBS density. The dotted curve was obtained from the dashed one by subtracting the LDA-X/UGBS oscillation profile. The exact potential was obtained by the method of ref 44.

in a complete basis set (or numerically), because the inversion in eq 2 is itself done analytically (in a complete basis). When the Kohn–Sham equations with a raw reconstructed potential are solved in a *finite* basis set, the resulting density will deviate from $\rho_{\text{input}}(\mathbf{r})$. This deviation may be very significant, especially when the raw reconstructed potential is highly oscillatory (as in Figures 1, 5, 7, and 8). Our smoothening scheme greatly reduces the density error in such cases.

Consider, for example, the PBE-XC/6-311G potentials for the Ne atom shown in Figure 5. The raw reconstructed potential is so inaccurate that the density obtained by solving (in a post-SCF fashion) the Kohn–Sham equations with this potential in the 6-311G basis set differs significantly from the original PBE-XC/6-311G density (Figure 10). After the raw

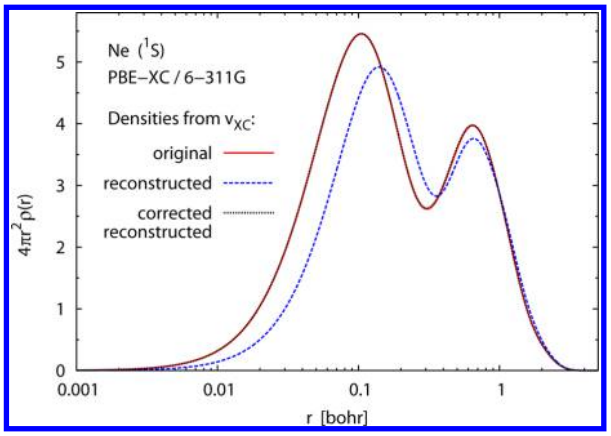

Figure 10. Radial electron densities for the Ne atom obtained from the PBE-XC/6-311G potentials of Figure 5 by solving the Kohn–Sham equations in the 6-311G basis. The solid and dotted curves are almost indistinguishable.

reconstructed potential is corrected by our method, it yields a density that virtually coincides with $\rho_{\text{input}}(\mathbf{r})$. Similar effects were observed for other systems and basis sets.

Note that Figure 10 shows a bad-case scenario in which the basis set is so small that the original and corrected reconstructed potentials do not agree perfectly. For larger basis sets such as u-6-311G and UGBS, where the original and corrected reconstructed potentials virtually coincide (as in Figures 6–9), the smoothening correction will cause the density error to vanish almost completely.

Exchange-correlation (and hence total) energies computed from electron densities generated by the reconstructed potentials are also vastly improved by the smoothening correction, especially in calculations with smaller basis sets (Table 1).

Table 1. Total PBE-XC Energies of the Ne Atom for the Electron Densities Generated by the PBE-XC Potentials Shown in Figures 5 and 6

	energy (E_h)	
PBE-XC potential	6-311G	UGBS
original	−128.834570	−128.866388
reconstructed	−124.130720	−127.175128
corrected reconstructed	−128.834271	−128.866388

6. CONCLUSION

Kohn–Sham potentials reconstructed from Gaussian-basis-set electron densities exhibit dramatic oscillations and asymptotic divergences. An efficient way to eliminate these artifacts is to generate the oscillation profile of some known potential (e.g., exchange-only LDA) for the basis set in which the reference density is expressed and then subtract this profile from the reconstructed potential. This method is particularly effective for medium-size basis sets. The correction is not just a visual improvement of potential curves—it largely eliminates the discrepancy between the input and output densities in finite-basis-set calculations with the reconstructed potentials.

We anticipate that the proposed remedy will greatly enhance the capabilities of existing density-to-potential mapping methods and density-embedding schemes. For example, Goodpaster et al.[17,18] recently described an exact density-embedding method in which both the Zhao–Morrison–Parr[24] procedure and the Kohn–Sham inversion formula are used to construct effective potentials for embedded subsystems. The resulting potentials exhibit spurious oscillations which can be removed by subtracting the corresponding LDA-X oscillation profiles. The smoothening should produce more realistic potentials and thereby improve the SCF convergence and numerical accuracy of the underlying density-embedding scheme.

Of course, in practical applications of Kohn–Sham inversion methods, there remains a greater challenge of how to efficiently construct Kohn–Sham potentials from densities for large, complex systems in the first place. Significant progress in that direction has been made recently in our ref 44, where we devised a robust method for constructing artifact-free exchange-correlation potentials from Hartree–Fock densities and densities corresponding to hybrid and kinetic-energy-density-dependent functionals.

AUTHOR INFORMATION

Corresponding Author

*E-mail: vstarove@uwo.ca.

Notes

The authors declare no competing financial interest.

ACKNOWLEDGMENTS

This work was supported by the Natural Sciences and Engineering Research Council of Canada (NSERC) through the Discovery Grants Program.

REFERENCES

(1) Kohn, W.; Sham, L. J. *Phys. Rev.* **1965**, *140*, A1133–A1138.
(2) Hohenberg, P. C.; Kohn, W.; Sham, L. J. *Adv. Quantum Chem.* **1990**, *21*, 7–26.

(3) Engel, E.; Dreizler, R. M. *Density Functional Theory: An Advanced Course*; Springer: Berlin, 2011.
(4) van Leeuwen, R.; Gritsenko, O. V.; Baerends, E. J. *Top. Curr. Chem.* **1996**, *180*, 107−167.
(5) Gritsenko, O. V.; Schipper, P. R. T.; Baerends, E. J. *Chem. Phys. Lett.* **1999**, *302*, 199−207.
(6) Becke, A. D.; Johnson, E. R. *J. Chem. Phys.* **2006**, *124*, 221101.
(7) Gaiduk, A. P.; Staroverov, V. N. *J. Chem. Phys.* **2008**, *128*, 204101.
(8) Staroverov, V. N. *J. Chem. Phys.* **2008**, *129*, 134103.
(9) Tozer, D. J.; Handy, N. C.; Green, W. H. *Chem. Phys. Lett.* **1997**, *273*, 183−194.
(10) Tozer, D. J.; Handy, N. C. *J. Chem. Phys.* **1998**, *108*, 2545−2555.
(11) Chan, G. K.-L.; Tozer, D. J.; Handy, N. C. *J. Chem. Phys.* **1997**, *107*, 1536−1543.
(12) Tozer, D. J.; Handy, N. C. *J. Phys. Chem. A* **1998**, *102*, 3162−3168.
(13) Handy, N. C.; Tozer, D. J. *Mol. Phys.* **1998**, *94*, 707−715.
(14) Menconi, G.; Wilson, P. J.; Tozer, D. J. *J. Chem. Phys.* **2001**, *114*, 3958−3967.
(15) Wesolowski, T. A. In *Computational Chemistry: Reviews of Current Trends*; Leszczynski, J., Ed.; World Scientific: Singapore, 2006; Vol. *10*, pp 1−82.
(16) Fux, S.; Jacob, C. R.; Neugebauer, J.; Visscher, L.; Reiher, M. *J. Chem. Phys.* **2010**, *132*, 164101.
(17) Goodpaster, J. D.; Ananth, N.; Manby, F. R.; Miller, T. F., III *J. Chem. Phys.* **2010**, *133*, 084103.
(18) Goodpaster, J. D.; Barnes, T. A.; Miller, T. F., III *J. Chem. Phys.* **2011**, *134*, 164108.
(19) Huang, C.; Carter, E. A. *J. Chem. Phys.* **2011**, *135*, 194104.
(20) de Silva, P.; Wesolowski, T. A. *J. Chem. Phys.* **2012**, *137*, 094110.
(21) van Leeuwen, R.; Baerends, E. J. *Phys. Rev. A* **1994**, *49*, 2421−2431.
(22) Gritsenko, O. V.; van Leeuwen, R.; Baerends, E. J. *Phys. Rev. A* **1995**, *52*, 1870−1874.
(23) Schipper, P. R. T.; Gritsenko, O. V.; Baerends, E. J. *Theor. Chem. Acc.* **1997**, *98*, 16−24.
(24) Zhao, Q.; Morrison, R. C.; Parr, R. G. *Phys. Rev. A* **1994**, *50*, 2138−2142.
(25) Tozer, D. J.; Ingamells, V. E.; Handy, N. C. *J. Chem. Phys.* **1996**, *105*, 9200−9213.
(26) Wu, Q.; Yang, W. *J. Chem. Phys.* **2003**, *118*, 2498−2509.
(27) Peirs, K.; Van Neck, D.; Waroquier, M. *Phys. Rev. A* **2003**, *67*, 012505.
(28) Kadantsev, E. S.; Stott, M. J. *Phys. Rev. A* **2004**, *69*, 012502.
(29) Ryabinkin, I. G.; Staroverov, V. N. *J. Chem. Phys.* **2012**, *137*, 164113.
(30) Mura, M. E.; Knowles, P. J.; Reynolds, C. A. *J. Chem. Phys.* **1997**, *106*, 9659−9667.
(31) Jacob, C. R. *J. Chem. Phys.* **2011**, *135*, 244102.
(32) King, R. A.; Handy, N. C. *Phys. Chem. Chem. Phys.* **2000**, *2*, 5049−5056.
(33) Kananenka, A. A.; Kohut, S. V.; Gaiduk, A. P.; Ryabinkin, I. G.; Staroverov, V. N.; unpublished.
(34) de Silva, P.; Wesolowski, T. A. *Phys. Rev. A* **2012**, *85*, 032518.
(35) Frisch, M. J.; Trucks, G. W.; Schlegel, H. B.; Scuseria, G. E.; Robb, M. A.; Cheeseman, J. R.; Montgomery, Jr., J. A.; Vreven, T.; Scalmani, G.; Mennucci, B.; Barone, V.; Petersson, G. A.; Caricato, M.; Nakatsuji, H.; Hada, M.; Ehara, M.; Toyota, K.; Fukuda, R.; Hasegawa, J.; Ishida, M.; Nakajima, T.; Honda, Y.; Kitao, O.; Nakai, H.; Li, X.; Hratchian, H. P.; Peralta, J. E.; Izmaylov, A. F.; Kudin, K. N.; Heyd, J. J.; Brothers, E.; Staroverov, V. N.; Zheng, G.; Kobayashi, R.; Normand, J.; Sonnenberg, J. L.; Iyengar, S. S.; Tomasi, J.; Cossi, M.; Rega, N.; Burant, J. C.; Millam, J. M.; Klene, M.; Knox, J. E.; Cross, J. B.; Bakken, V.; Adamo, C.; Jaramillo, J.; Gomperts, R.; Stratmann, R. E.; Yazyev, O.; Austin, A. J.; Cammi, R.; Pomelli, C.; Ochterski, J. W.; Ayala, P. Y.; Morokuma, K.; Voth, G. A.; Salvador, P.; Dannenberg, J. J.; Zakrzewski, V. G.; Dapprich, S.; Daniels, A. D.; Strain, M. C.; Farkas, O.; Malick, D. K.; Rabuck, A. D.; Raghavachari, K.; Foresman, J. B.; Ortiz, J. V.; Cui, Q.; Baboul, A. G.; Clifford, S.; Cioslowski, J.; Stefanov, B. B.; Liu, G.; Liashenko, A.; Piskorz, P.; Komaromi, I.; Martin, R. L.; Fox, D. J.; Keith, T.; Al-Laham, M. A.; Peng, C. Y.; Nanayakkara, A.; Challacombe, M.; Chen, W.; Wong, M. W.; Pople, J. A. *Gaussian Development Version*, Revision F.02; Gaussian, Inc.: Wallingford, CT, 2006.
(36) de Castro, E. V. R.; Jorge, F. E. *J. Chem. Phys.* **1998**, *108*, 5225−5229.
(37) Indeed, the asymptotic tail of the density is dominated by the basis function with the smallest exponent. If this function is a Gaussian, $g(r) \propto \exp(-\alpha r^2)$, then by inverting the one-electron Schrödinger equation with a centrally symmetric potential $v_{\text{eff}}(r)$ we find that $v_{\text{eff}}(r) = 2\alpha^2 r^2 - 3\alpha + E$, where E is a constant. In the asymptotic region of a neutral atom, $v_{\text{H}}(r) + v(r) \approx 0$, so $v_{\text{eff}}(r) \approx v_{\text{XC}}(r)$. In the case of the Ne atom, we have verified that the potential $v_{\text{eff}}(r)$ for the most diffuse s-type function of the 6-311G basis set[38] (α = 0.3970570) accurately reproduces the parabolic tail of the reconstructed LDA-X potential shown in Figure 1.
(38) Schuchardt, K. L.; Didier, B. T.; Elsethagen, T.; Sun, L.; Gurumoorthi, V.; Chase, J.; Li, J.; Windus, T. L. *J. Chem. Inf. Model.* **2007**, *47*, 1045−1052.
(39) Perdew, J. P.; Burke, K.; Ernzerhof, M. *Phys. Rev. Lett.* **1996**, *77*, 3865−3868; **1997**, *78*, 1396(E).
(40) Frisch, A.; Frisch, M. J.; Trucks, G. W. *Gaussian 03 User's Reference*, 2nd ed.; Gaussian, Inc.: Wallingford, CT, 2005.
(41) Baltin, R. *Phys. Lett. A* **1986**, *117*, 317−324.
(42) Holas, A.; March, N. H. *Int. J. Quantum Chem.* **1995**, *56*, 371−383.
(43) Ryabinkin, I. G.; Staroverov, V. N. *Int. J. Quantum Chem.* **2013**, *113*, 1626−1632.
(44) Ryabinkin, I. G.; Kananenka, A. A.; Staroverov, V. N. *Phys. Rev. Lett.* **2013**, *111*, 013001.